Bio-Medical Materials and Engineering 24 (2014) 1979–1989
DOI 10.3233/BME-141007
IOS Press

Preparation and characterization of polyurethane/soluble eggshell membrane nanofibers

Long Chen[a,b], Jian Kang[c] and Sachiko Sukigara[c,*]
[a]*State Key Laboratory for Modificaion of Chemical Fibers and Polymer Materials, Donghua University, 2999 Renmin Rd. North, Shanghai 201620, China*
[b]*Center for Fiber and Textile Science, Kyoto Institute of Technology, Matsugasaki, Sakyo-ku, Kyoto 606-8585, Japan*
[c]*Department of Advanced Fibro-Science, Graduate School of Science and Technology, Kyoto Institute of Technology, Matsugasaki, Sakyo-ku, Kyoto 606-8585, Japan*

Abstract. Superfine Particles (SP) of soluble eggshell membrane and medical grade polyurethane (MPU) blend nanofibers were prepared by electrospinning different blend ratios of SP/MPU suspensions for regeneration of the natural fiber-like structure of the eggshell membrane. The addition of SP had no obvious effect on the electrospinning process of MPU nanofibers, and the SP were randomly dispersed in the MPU nanofibers with no agglomeration of SP when the amount of SP was less than 20 wt%. Although the average diameter of the blend nanofibers is approximately 30% larger than that of the pure MPU nanofibers, they exhibit excellent tensile strength and tensile resilience that are close to those for pure MPU nanofibers. In addition, the blend nanofibers become fully hydrophilic, and the water contact angle of the blend nanofibers decreases dramatically to 0°. Therefore, with the advantages of a collagen ingredient and good hydrophilicity, these blend nanofibers are suitable for applications such as facial masks, wound dressings, and pharmaceutical carrier materials.

Keywords: Egg shell membrane, polyurethane, nanofibers, mechanical properties, morphology

1. Introduction

Eggshell membrane (ESM), which constitutes approximately 1.02 wt% of a hen egg, contains about 90 wt% collagen, 3 wt% lipid, and 2 wt% sugar and is an abundant natural proteinous resource that has been used as an effective traditional Chinese external medicine named ‘coating for phoenix’ for the treatment of burns and ulcers [1,2]. ESM is similar to natural extracellular matrix (ECM), in that it has a highly porous structure of interwoven protein fibers, surrounding the egg yolk which is an ovum cell [3,4]. It has been used as a biomaterial, particularly as a matrix for biosorption of heavy metal ions [5], a template for the formation of ordered tube networks [6], a platform for enzyme immobilization

*Corresponding author: Sachiko Sukigara, Department of Advanced Fibro-Science, Graduate School of Science and Technology, Kyoto Institute of Technology, Matsugasaki, Sakyo-ku, Kyoto 606-8585, Japan. Tel.: 0081-75-7247365; E-mail: sukigara@kit.ac.jp.

[7], and as a scaffold material for tissue engineering [8]. However, natural ESM is neither soluble nor fusible, so that the reformation of natural ESM into various shapes and sizes is difficult. Soluble ESM (SESM) is prepared from ESM using reduction dissolved method, which has good bioactive protein [9]. Rather than employing natural ESM, soluble ESM has been considered for different applications.

However, SESM is also difficult to form into different shapes and sizes, and even if it could be formed into film or fiber, its mechanical properties will be very poor due to its low molecular weight and wide molecular weight dispersion [10]. Therefore, recent research has focused on blending ESM with water-soluble polymers such as poly (vinyl alcohol) (PVA) and poly (ethylene oxide) (PEO) and then processing it into fibers or films with simultaneous cross-linking to make it insoluble [11,12], or grafting ESM onto the surface of water-insoluble polymers, such as polycaprolactone (PCL) or polyethylene (PE) fiber or film [13,14], to generate the natural fiber-like structure of ESM. However, either the processes for the preparation of such fibers or films were too complicated or the resultant mechanical properties were poor, and the products were usually insoluble and not suitable for applications such as facial masks, wound dressings and pharmaceutical carriers. SESM can be made into superfine particles with excellent hydrophilicity, which is an important performance requirement of wound dressings, facial masks and other biomaterials [15]. Therefore, SESM can be blended directly with nontoxic polymers that possess good mechanical properties and then formed into nanofibers, which has significant potential for applications in wound dressings, facial masks and pharmaceutical carrier materials.

Polyurethane (PU), a polymer material developed in the 1930s, offers high strength, good wear resistance, tear resistance, flexibility, oil resistance, and excellent blood compatibility. Foam, plastic, elastomers, paints, adhesive materials, elastic fibers, and synthetic leather made from PU resin play an important role in modern industries [16]. In particular, PU can be easily formed into nanofiber webs by electrospinning, which have significant potential for applications such as separation filters, wound dressing materials, tissue scaffolds, and sensors [17–27]. However, to overcome the disadvantageous properties of traditional and pure PU products, such as hydrophobicity, superfine particles (SP) are widely applied in the modification of PU products [28–32]. Unlike traditional research on the modification of PU products using inorganic nanoparticles, in this study, nanofibers were prepared from a blend of SESM superfine particles (SP) and medical grade PU (MPU) to reduce the hydrophobicity and realize the application of SESM as a biomaterial. The morphology, structure, surface wettability and mechanical properties of the MPU-SP blend nanofibers were investigated.

2. Experiment

2.1. Materials

SP of SESM (Idemitsu Technofine Co., Ltd, Mw =6000, average diameter 2 μm) and MPU (Fluka, Selectophore ®, 81367-5G) were used as starting materials. Acetone (Nacalai Tesque) and dimethylacetamide (DMAc; Wako) were used as solvents for MPU.

2.2. Electrospinning

MPU was dissolved at 12 wt% in a DMAc/acetone (60/40 w/w) co-solvent under stirring for 24 h at room temperature. MPU-SP suspensions with various weight ratios (95:5, 90:10, 85:15 and 80:20, denoted as MPU-SP 5, MPU-SP 10, MPU-SP 15 and MPU-SP 20, respectively) were prepared by add-

ing appropriate amounts of SP to the MPU solution and then stirring for 24 h at room temperature. MPU-SP suspensions were placed into a 2.5 mL syringe capped with a 22-gauge blunt end needle and mounted in a syringe pump (KD Scientific, 780,100E). The positive lead from a high voltage supply (Gamma High Voltage Research Inc., E S40P-20W) was attached via an alligator clip to the external surface of the metal syringe needle. A square (8×8 cm2) grounded target fabricated from stainless steel was mounted 15 cm from the tip of the syringe tip. At the onset of electrospinning, the syringe pump was set to deliver the source solution at a rate of 0.4 mL/h. A high voltage of 15 kV was simultaneously applied across the source solution and the grounded target mandrel. All nanofibers for characterization were prepared by electrospinning for 1 h followed by vacuum drying for 24 h.

2.2.1. Characterization

Morphological observations of the MPU-SP nanofibers were conducted using a field emission scanning electron microscope (FE-SEM; Hitachi, 4200) at an acceleration voltage of 8 kV. For each sample, fiber diameter was measured at 50 different points using Image J 1.42q. software.

The water contact angle (WCA) was measured using a contact angle tester (Kyowa Interface Science Co., Ltd., CA-S150). Then 4 μL of deionized water was dropped onto the surface of electrospun nanofiber webs at 24°C and 60% relative humidity. The WCA was measured using Image J 1.42q. software.

Tensile strength tests were performed at room temperature using a micro-tensile tester (Kato Tech Co., Ltd., KES-G5S). The micro-tensile tester was set up with a 0.5 cm gauge length and a crosshead speed of 0.1 cm/s. The length and width of the test samples were both 1 cm. Tensile resilience was obtained at a crosshead speed of 0.1 cm/s and a maximum load of 0.1 N/cm with ten-cycle tests; the length and width of the samples were both 1 cm. For each sample, at least five specimens were tested.

The composition of the nanofibers was observed using Fourier transform infrared spectroscopy (ATR-FTIR PerkinElmer, Spectrum GX) in the wavenumber range of 700-4000 cm^{-1} with a resolution of 8 cm^{-1}. Each measurement was composed of an average of 16 scans.

3. Results and discussion

3.1. Morphology

The formation of uniform MPU-SP nanofibers from suspension was continuous and stable when the weight ratio of SP to MPU was less than 20:80, where the SP were evenly distributed throughout the MPU solution. FE-SEM images (see Figure 1) of the electrospun nanofibers also confirmed that electrospun MPU-SP nanofibers formed using these weight ratios were uniform. SP are randomly dispersed in the MPU nanofibers with no agglomeration of SP when the weight ratio of SP to MPU is less than 20:80, which indicates that there is at least a strong interaction force between SP and MPU in the nanofibers. However, when the weight ratio of SP to MPU was 20:80, SP were unevenly distributed in the MPU nanofibers, though confined. Moreover, as shown in Figure 2 and Table 1, with the increasing weight ratio of SP, although the average diameters of the nanofibers increased from 972 nm, which was the average diameter of pure MPU nanofibers, to above 1200 nm, the morphology of MPU-SP nanofibers remained the same, and the variation tendency of the diameter of MPU-SP nanofibers was not obvious due to the wide diameter distribution. The increase of the diameter is probably due to the higher viscosity of the spinning solution than pure MPU spinning solution caused by the interaction between MPU and SP [27], which also has a probable effect on the mechanical properties.

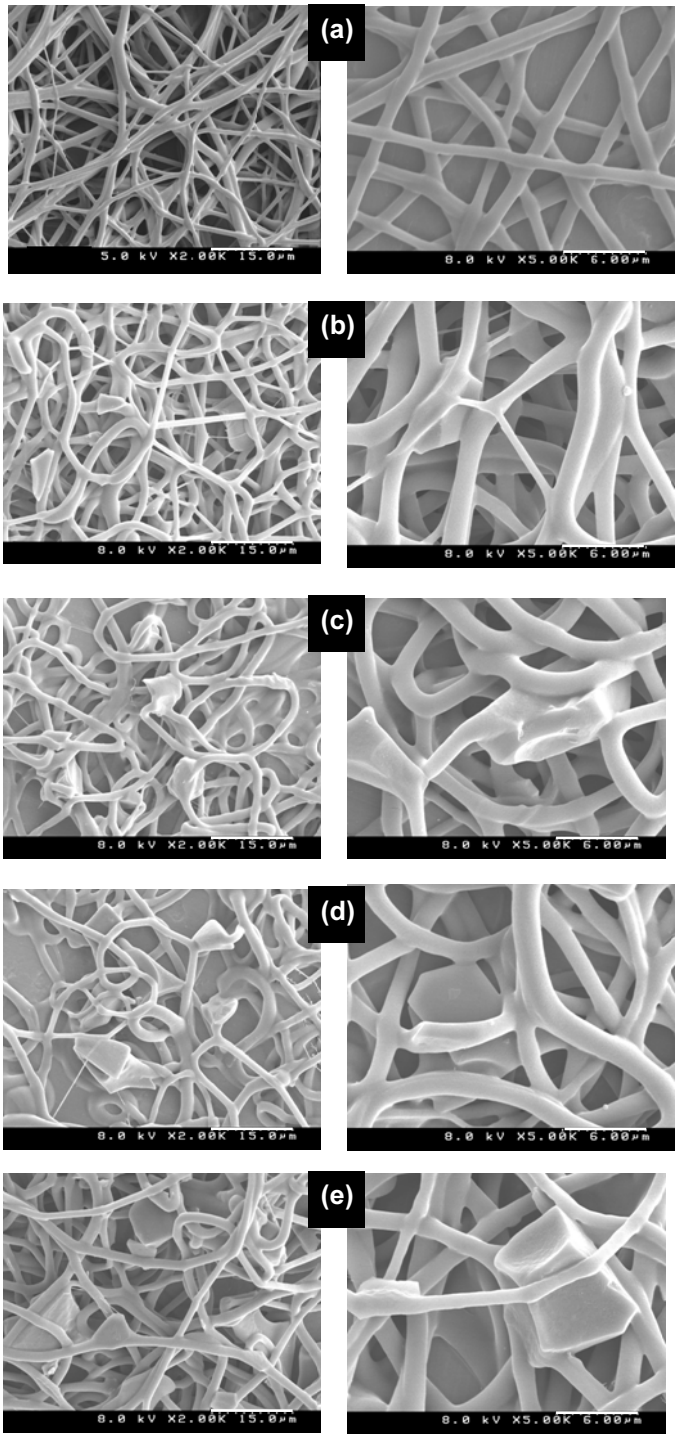

Fig. 1. FE-SEM images of different nanofibers of (a) MPU, (b) MPU-SP 5, (c) MPU-SP 10, (d) MPU-SP 15 and (e) MPU-SP 20.

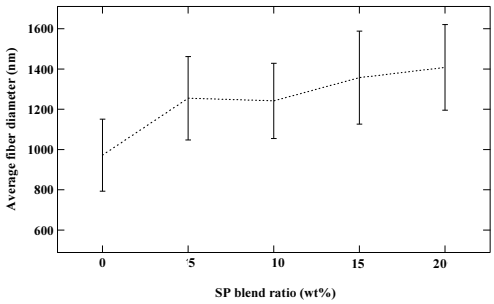

Fig. 2. The average diameters of MPU-SP nanofibers.

Table 1

The average diameters of MPU-SP nanofibers

Samples	MPU	MPU-SP 5	MPU-SP 10	MPU-SP 15	MPU-SP 20
Diameter (nm)	972±179	1255±207	1242±187	1357±231	1408±213

3.2. Wettability

To investigate the wettability of MPU-SP nanofiber webs, the WCAs were measured, and the results are given in Figure 3 and Table 2. The WCAs of MPU nanofiber webs decreased from 112.4° to 0° after the addition of SP at SP:MPU weight ratios less than 20:80. The WCA does not vary with the variation of the SP:MPU weight ratio at less than 20:80, because the blends are fully hydrophilic as a result of the excellent water solubility of SP. However, when the SP:MPU weight ratio is 20:80, the WCA of the MPU-SP blend nanofiber web is very small, but fluctuates widely due to the uneven dispersion of SP, which is evident in Figure 1.

3.3. Mechanical properties

3.3.1. Tensile strength

For the tensile strength tests, the sample of 1 cm wide was used as the initial loading unit to calculate the tensile load and Young's modulus, considering the precise thickness of the nanofiber webs was difficult to be measured. Stress-strain curves of MPU-SP nanofiber webs are shown in Figure 4, and the tensile properties of MPU-SP nanofiber webs obtained from these stress-strain curves are summarized in Table 3. The tensile strength at break and elongation at break for MPU-SP nanofiber webs show the maximum extension under the testing conditions. All the MPU-SP nanofiber webs exhibit excellent mechanical properties similar to those of pure MPU nanofibers. After the addition of SP, the tensile strength at break is lower and the elongation at break and Young's modulus are higher compared with pure MPU nanofiber webs. Moreover, the tensile strength at break, elongation at break and Young's modulus of the MPU-SP nanofibers first increase with the increasing weight ratio of SP to MPU, and then decrease. It was reported that the geometrical arrangement of electrospun nanofibers and the density and distribution of bonded points in nanofiber mats have a significant effect on the mechanical behavior of electrospun nanofiber mats [33]. In the present study, these factors are mainly affected by both the diameters of the MPU nanofibers and the distribution and the number of SP. The

diameters of all MPU-SP nanofibers are larger than those of pure MPU nanofibers, and as the amount of SP increases, SP are firstly distributed evenly in the MPU nanofibers and act as physical crosslink

Table 2

Contact angle values of M-PU-SP nanofiber webs

Samples	M-PU	M-PU-SP 5	M-PU-SP 10	M-PU-SP 15	M-PU-SP 20
Contact(°)	112.4±0.5	0	0	0	Fluctuate widely

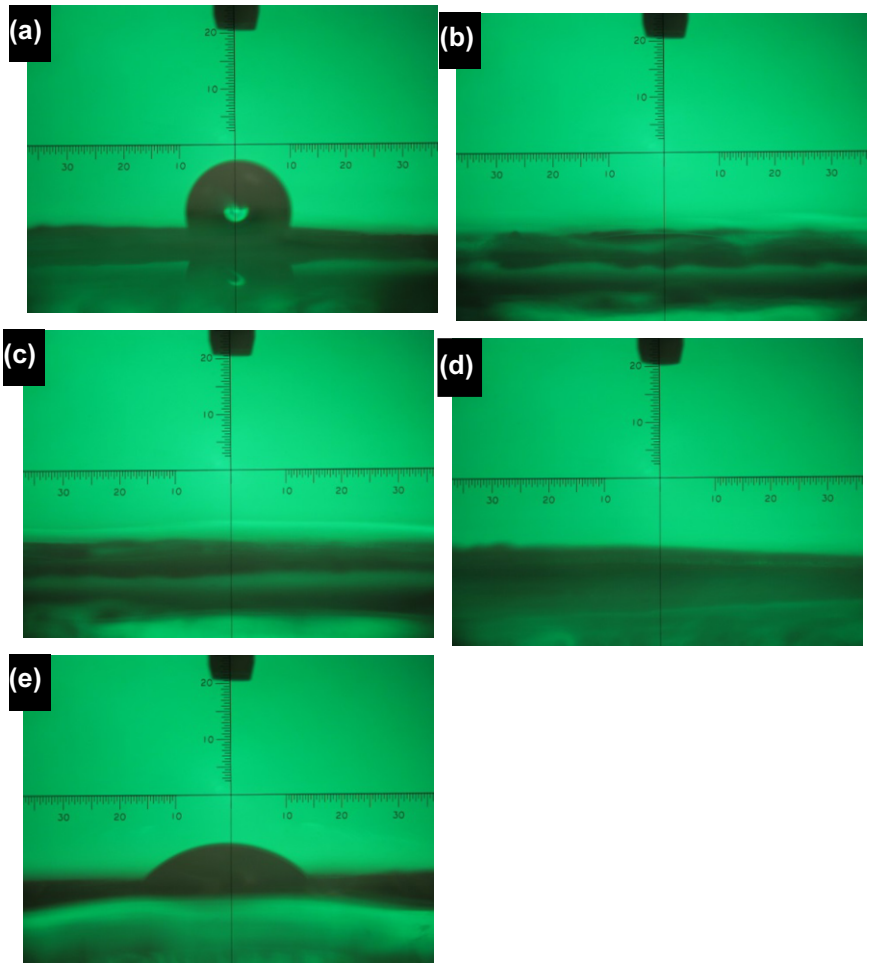

Fig. 3. Contact angle pictures of different nanofibers of (a) MPU, (b) MPU-SP 5, (c) MPU-SP 10, (d) MPU-SP 15 and (e) MPU-SP 20.

ing points. However, although a greater amount of SP result in uneven distribution, weak spots, a change in the tensile strength at break, SP are more rigid than MPU and act as a “lubricant” between the MPU nanofibers, leading to the increase of Young’s modulus and elongation at break.

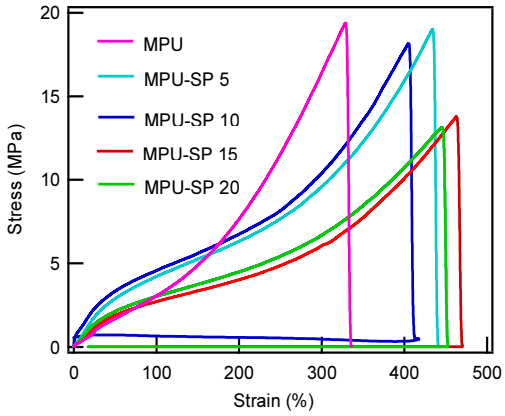

Fig. 4. Strain-stress curves of MPU-SP nanofiber webs.

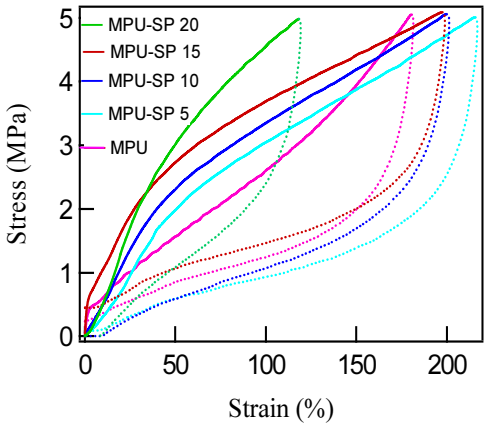

Fig. 5. Typical resilience curves of MPU-SP nanofiber webs for the first load-extension testing.

3.3.2. Tensile resilience

As is well known, the flexibility of a material is not only dependent on its extensibility, but also on its resilience. According to the results for the tensile properties, MPU-SP blend nanofiber webs show higher extensibility than pure MPU nanofiber webs. The resilience properties of the test samples were measured by cyclic tensile tests. Typical resilience (RT) curves of MPU-SP nanofiber webs prepared using different ratios of SP to MPU are shown in Figures 5 and 6, and the tensile properties obtained from these curves are summarized in Table 4. The RT values of the blend nanofiber webs for the first load-extension testing (Figure 5) are slightly lower than those of pure MPU nanofiber webs and increase then decrease with the increasing weight ratio of SP to MPU. The average RT values of the blend nanofiber webs for the 10 cycle tests are very similar to those of the pure MPU nanofiber webs. This confirms that the blend nanofiber webs have similar excellent resilience to that of pure MPU nanofiber webs and the addition of SP does not obviously affect the resilience property. At maximum extension, the same variation tendency to that above elongation at break is observed. This difference in resilience results from the interaction between SP and MPU, where SP act as physical crosslinking points of MPU nanofibers, which varies according to the variation of SP distribution and number.

Table 3

Mechanical parameters of MPU-SP nanofiber webs

Samples	Tensile strength at break (Mpa)	Elongation at break (%)	Young's modulus (Mpa)
MPU	18.63±0.92	327±17	4.65±0.25
MPU-SP5	16.76±1.42	405±38	5.12±0.35
MPU-SP10	17.88±1.42	431±19	5.22±0.09
MPU-SP15	14.02±0.27	453±23	4.87±0.16
MPU-SP20	13.9±0.36	434±22	4.90±0.38

Table 4

Resilience properties of MPU-SP nanofiber webs for the first load-extension testing

Samples	Maximum extension (%)		WT[a] $\times 10^{-2}$(J/m^2)		RT[b] (%)	
	The first load	10 repeat tests	The first load	10 repeat tests	The first load	10 repeat tests
MPU	181±5	214±15	45.2±2.3	32.6±4.4	53.3±3.6	71.2±6.8
MPU-SP5	216±9	283±36	64.1±3.1	48.1±5.8	39.3±2.5	67.5±9.9
MPU-SP10	200±7	252±29	62.5±2.7	48.3±5.2	39.3±2.7	69.7±10.7
MPU-SP15	197±6	290±44	67.9±4.5	50.7±6.3	46.0±3.1	64.2±7.3
MPU-SP20	118±4	152±18	35.8±2.2	30.1±2.8	45.7±2.8	72.9±9.7

[a]Tensile energy.
[b]Tensile resilience.

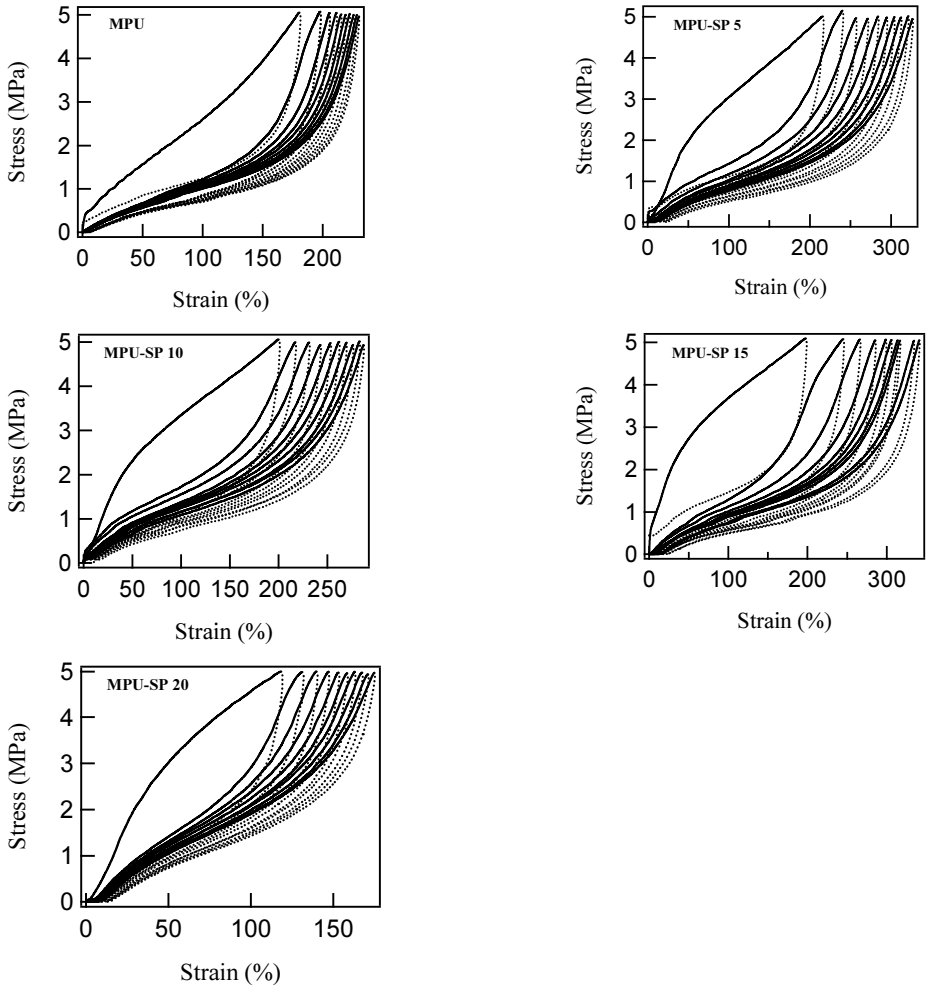

Fig. 6. Typical resilience curves of MPU-SP nanofiber webs with 10 repeat tests.

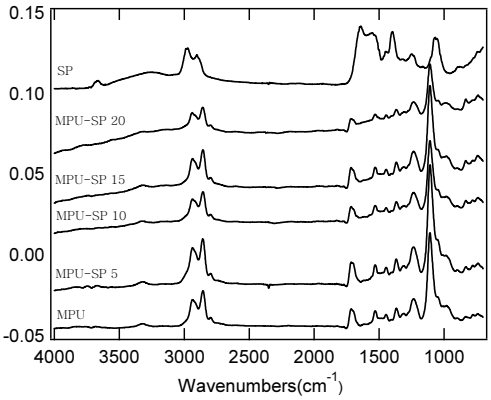

Fig. 7. FTIR curves of MPU-SP nanofibers.

3.4. FTIR analysis

It has been reported that strong hydrogen bonding between NH and C=O is formed in protein and PU [34]. SP distribute in the MPU nanofibers as particles and its functional groups are similar to that of MPU, so the peaks shifts caused by hydrogen bonds is very weak and cannot be observed in the FTIR spectra (see Figure 7). However, the results for the electrospinnability and morphology of the MPU-SP blend nanofibers indicate that there is a chemical interaction between SP and MPU.

4. Conclusion

SP have a good compatibility with the MPU solution, and the resultant blends have good electrospinnability. The addition of SP has no obvious effect on the electrospinning process of MPU nanofibers, although the average diameter of MPU-SP nanofibers is larger than that of pure MPU nanofibers and increases with the increasing SP weight ratio. There is strong physical interaction between SP and MPU nanofibers, because SP are distributed randomly in the MPU nanofibers with no agglomeration of SP and act as physical crosslinking points so that SP do not affect the mechanical properties of MPU-SP nanofibers, but their hydrophilicity is enhanced significantly. Therefore, these nanofiber blends have significant potential for applications such as facial masks, wound dressings, and pharmaceutical carrier materials.

Acknowledgment

The authors acknowledge the Fundamental Research Funds for the Central Universities (Project No. 2232013A3-02) for financial support.

References

[1] R.Y. Zhang and J.C. Chen, Studies on extracting keratin in the eggshell membrane, Food Sci. **26** (2005), 251–254.
[2] Q.X. Kui and Z.L. Zhang, Sixteen patients with skin chronic ulcer treated externally by using Han's egg endomembrane and Chinese herbal medicine, China's Naturopathy **11** (2003), 29–30.

[3] T. Nakano, N.I. Ikawa and L. Ozimek, Chemical composition of chicken eggshell and shell membranes, Poult. Sci. **82** (2003), 510–514.
[4] W.T. Tsai, J.M. Yang, C.W. Lai, Y.H. Cheng, C.C. Lin and C.W. Yeh, Characterization and adsorption properties of eggshells and eggshell membrane, Bioresour. Technol. **97** (2006), 488–493.
[5] K. Suyama, Y. Fukazawa and Y. Umetsu, A new biomaterial, hen eggshell membrane, to eliminate heavy metal ion from their dilute waste solution, Appl. Biochem. Biotechnol. **45/46** (1994), 871–879.
[6] D. Yang, L. Qi and J. Ma, Eggshell membrane templating of hierarchically ordered macroporous networks composed of TiO2 tubes, Adv. Mater. **14** (2002), 1543–1546.
[7] D. Xiao and M.M.F. Choi, Aspartame optical biosensor with bienzyme-immobilized eggshell membrane and oxygen-sensitive optode membrane, MFC Anal. Chem. **74** (2002), 863–870.
[8] T. Ino, M. Hattori, T. Yoshida, S. Hattori, K. Yoshimura and K. Takahashi, Improved physical and biochemical features of a collagen membrane by conjugating with soluble egg shell membrane protein, Biosci. Biotechnol. Biochem. **70** (2006), 865–873.
[9] F. Yi, J. Yu, Z. Guo, L. Zhang and Q. Li, Natural bioactive material: a preparation of soluble eggshell membrane protein, Macromol. Biosci. **3** (2003), 234–237.
[10] J. Kang, M. Kotaki, S. Okubayashi and S. Sukigara, Fabrication of electrospun eggshell membrane nanofibers by treatment with catechin, J. Appl. Polym. Sci. **117** (2010), 2042–2049.
[11] X. Xiong, Q. Li, F. Yi, J. Lu, Z. Guo and J. Yu, Application of eggshell membrane protein in biocompatible materials, Polym. Bull., 2011, 25–33.
[12] F. Yi, J.W. Lu, Z.X. Guo and J. Yu, Mechanical properties and biocompatibility of soluble eggshell membrane protein/poly(vinyl alcohol) blend films, J. Biomater. Sci. Polym. Ed. **17** (2006), 1015–1024.
[13] F. Yi, Q. Li, Z.X. Guo and J. Yu, Immobilization of soluble eggshell membrane protein on polyethylene film surface: Effect on the culture of NIH3T3in vitro, J. Appl. Polym. Sci. **99** (2006), 1340–1345.
[14] J. Jia, Y.Y. Duan, J. Yu and J.W. Lu, Preparation and immobilization of soluble eggshell membrane protein on the electrospun nanofibers to enhance cell adhesion and growth, J. Biomed. Mater. Res. Part A **86A** (2008), 364–373.
[15] B.D. Ratner, A.S. Hoffman, F.J. Schoen and J.E. Lemons, Biomaterials science: an introduction to materials in medicine, Academic Press, San Diego, 1996, pp. 57–59.
[16] Y.P. Wei, F. Cheng, H.P. Li and J.G. Yu, Synthesis and properties of polyurethane resins based on liquefied wood, J. Appl. Polym. Sci. **92** (2004), 351–356.
[17] M.M. Demir, I. Yilgor, E. Yilgor and B. Erman, Electrospinning of polyurethane fibers, B Polymer **43** (2002), 3303–3309.
[18] A. Pedicini and R.J. Farris, Mechanical behavior of electrospun polyurethane, Polymer **44** (2003), 6857–6862.
[19] D.I. Cha, H.Y. Kim, K.H. Lee, Y.C. Jung, J.W. Cho and B.C. Chun, Electrospun nonwovens of shape-memory polyurethane block copolymers, J. Appl. Polym. Sci. **96** (2005), 460–465.
[20] J.J. Guan, K.L. Fujimoto, M.S. Sacks and W.R. Wagner, Preparation and characterization of highly porous, biodegradable polyurethane scaffolds for soft tissue applications, Biomaterials **26** (2005), 3961–3971.
[21] M.G. Mckee, T. Park, S. Unal, I. Yilgor and T.E. Long, Electrospinning of linear and highly branched segmented poly (urethane urea)s, Polymer **46** (2005), 2011–2015.
[22] Z.M. Huang, Y.Z. Zhang, M. Kotaki and S. Ramakrishna, A review on polymer nanofibers by electrospinning and their applications in nanocomposites, Compos. Sci. Technol. **63** (2003), 2223–2253.
[23] H.S. Park and P. Young, Filtration properties of electrospun ultrafine fiber webs, Korean J. Chem. Eng. **22** (2005), 165–172.
[24] L. Huang, K. Nagapudi, R.P. Apkarian and E.L. Chaikof, Engineered collagen-PEO nanofibers and fabrics, J. Biomater. Sci. Polym. Ed. **12** (2001), 979–993.
[25] X.Y. Wang, C. Drew, S.H. Lee, K.J. Senecal, J. Kumar and L.A. Samuelson, Electrospun Nanofibrous Membranes for Highly Sensitive Optical Sensors, Nano. Lett. **2** (2002), 1273–1275.
[26] W.J. Li, C.T. Laurencin, E.J. Caterson, R.S. Tuan and F.K. Ko, Electrospun nanofibrous structure: a novel scaffold for tissue engineering, J. Biomed. Mater. Res. **60** (2002), 613–621.
[27] J.A. Matthews, G.E. Wnek, D.G. Simpson and G.L. Bowlin, Electrospinning of Collagen Nanofibers, Biomacromolecules **3** (2002), 232–238
[28] J.A. Mikroyannidis, Polyesters, polyurethanes, and epoxy resin derived from 2,2′-(1,4–phenylenedivinylene)bis-5-hydroxypyridine, J. Polym. Sci. Part A: Polym. Chem. **29** (1991), 881–887.
[29] D. Feldman, Modification of the properties of polyurethane by blending, reinforcing, or plasticizing, J. Appl. Polym. Sci. **27** (1982), 1933–1944.
[30] A. Pattanayak and S.C. Jana, Synthesis of thermoplastic polyurethane nanocomposites of reactive nanoclay by bulk polymerization methods, Polymer **46** (2005), 3275–3288.

[31] X. Cao, L. James Lee, T. Widya and C. Macosko, Polyurethane/clay nanocomposites foams: processing, structure and properties, Polymer **46** (2005), 775–783.
[32] J.S. Ma, S.F. Zhang and Z.N. Qi, Synthesis and Characterization of Elastomeric Polyurethane/Clay Nanocomposites, J. Appl. Polym. Sci. **82** (2001), 1444–1448.
[33] K.H. Lee, H.Y. Kim, Y.J. Ryu, K.W. Kim and S.W. Choi, Mechanical behavior of electrospun fiber mats of poly (vinyl chloride)/polyurethane polyblends, J. Polym. Sci. Part B: Polym. Phys. **41** (2003), 1256–1262.
[34] N.G. Wang and L.N. Zhang, Preparation and characterization of soy protein plastics plasticized with waterborne polyurethane, Polym. Int. **54** (2005), 233–239.